Structural Model for the Reaction Mechanism of Glutamine Synthetase, Based on Five Crystal Structures of Enzyme–Substrate Complexes‡

Shwu-Huey Liaw§ and David Eisenberg*

UCLA-DOE Lab of Structural Biology and Molecular Medicine, Molecular Biology Institute and Department of Chemistry and Biochemistry, University of California, Los Angeles, California 90024-1570

Received July 8, 1993; Revised Manuscript Received October 12, 1993●

ABSTRACT: Glutamine synthetase brings nitrogen into metabolism by condensing ammonia and glutamate, with the aid of ATP, to yield glutamine, ADP, and inorganic phosphate. Here we present five crystal structures of GS complexed with each of two substrates, Glu and AMPPNP (an ATP analog), with a transition-state analogue, L-methionine-*S*-sulfoximine, and with each of two products, Gln and ADP. GS of the present study is from *Salmonella typhimurium*, has Mn^{2+} bound, and is fully unadenylylated. Protein–metal–substrate interactions and small but significant conformational changes induced by substrate binding are defined by Fourier maps. On the basis of these maps, we propose a tentative structure-based enzymatic mechanism of glutamine synthesis with these steps: (1) ATP binds first at the top of the funnel-shaped active site cavity, adjacent to the n_2 Mn^{2+}; Arg 359 moves toward the Glu binding site. (2) Glu binds adjacent to the n_1 Mn^{2+} at the bottom of the active site near a flexible loop (residues 324–328). As proposed earlier by Meister and others, Glu attacks the γ-phosphorus atom of ATP to produce γ-glutamyl phosphate and ADP. (3) The presence of ADP (but not ATP) moves Arg 339 toward the P_i site, perhaps stabilizing the γ-glutamyl phosphate, and moves Asp 50′ of the adjacent subunit toward a putative ammonium ion site, enhancing binding of this third substrate. Deprotonation of the ammonium ion, perhaps by Asp 50′, permits the resulting active species, ammonia, to attack the γ-glutamyl phosphate, forming a tetrahedral intermediate. (4) This tetrahedral intermediate stabilizes the Glu binding loop, residues 324–328, because of the interaction of the positive charge on the γ-amino group of the intermediate with the negative charge on the side chain of Glu 327, closing the path of Glu entry through the bottom of the active site funnel. (4) Phosphate leaves through the top of the active site and a proton from the γ-amino group of the tetrahedral intermediate is lost, perhaps to Glu 327, to yield Gln. The absence of electrostatic interaction between Glu 327 and the product Gln permits the segment (residues 324–328) to open, allowing Gln to leave through the bottom of the active site and Glu to enter for the next catalytic cycle. These five crystal structures of GS–substrate complexes also suggest possible mechanisms for other reactions catalyzed by GS.

Glutamine synthetase (GS)[1] regulates cellular nitrogen metabolism in microorganisms, animal tissues, and plants. It catalyzes the biosynthesis of glutamine from ammonia, glutamate, and ATP in what is termed the "biosynthetic reaction". Glutamine then serves as the source of nitrogen in the biosynthesis of many other compounds. GS also provides a mechanism for ammonia assimilation and detoxification and a mechanism for termination of neurotransmitter signals in tissues where glutamate acts as a neurotransmitter (Cooper & Plum, 1987; Derouiche & Frotscher, 1991).

The reactions catalyzed by bacterial dodecameric GS (prokaryote GSI) (Stadtman & Ginsburg, 1974) and mammalian octameric GS (eukaryote GSII) (Meister, 1974) are generally the same. In addition to the biosynthetic reaction, glutamine hydrolysis by GS into glutamate and ammonia in the presence of the cofactors ADP and P_i may be important in the production of ammonia and in the maintenance of proper acid–base balance. Glutamine hydrolysis is accelerated by replacement of phosphate with arsenate ("arsenolysis of glutamine"). Hydroxylamine can replace ammonia in the biosynthetic reaction forming γ-glutamylhydroxamate. Also, GS catalyzes γ-glutamyl transfer from Gln to hydroxylamine yielding γ-glutamylhydroxamate, termed the "γ-glutamyl transfer reaction". Still other reactions catalyzed by GS have been described by Whitley and Ginsburg (1980).

Similar catalytic reaction mechanisms have been proposed for GS from both eukaryotes and prokaryotes (Meister, 1980; Meek & Villafranca, 1980). In both, glutamine synthesis is believed to proceed a two-step process. Studies of the tight-binding inhibitor MetSox suggested that the reaction is not concerted but instead proceeds through an enzyme-bound intermediate. Irreversible inhibition of GS by MetSox in the presence of ATP and Mg^{2+} or Mn^{2+} was first shown by Meister and co-workers, who suggested the formation of a GS-bound γ-glutamyl phosphate and a transient tetrahedral intermediate whose structure is analogous to that of MetSox-P (Figure 1) (Weisbrod & Meister, 1973). Also, GS inactivation by various ATP analogs in the presence of Mn^{2+} and MetSox showed formation of an ADP analog and MetSox-P (Maurizi & Ginsburg, 1986).

Thus much is known of the chemical steps in the biosynthesis of glutamine, but the structural basis of these steps is still largely undefined. For example, still undefined is the structural basis of the interactions of protein and substrates, including the binding of ammonium ion or ammonia, the involvement of specific GS residues, and the roles of the two enzyme-bound metal ions in catalytic processes.

* To whom correspondence should be addressed.

‡ The glutamine synthetase coordinates used here for computing difference maps have been deposited with the Brookhaven Protein Data Bank with the identity code 1 LGS.

§ Present address: Institute of Molecular Medicine, School of Medicine, National Taiwan University, Taipei, Taiwan.

● Abstract published in *Advance ACS Abstracts*, December 1, 1993.

[1] Abbreviations: GS, glutamine synthetase; AMPPNP, 5′-adenylylimide diphosphate; MetSox, L-methionine-*S*-sulfoximine; MetSox-P, L-methionine-*S*-sulfoximine phosphate.

0006-2960/94/0433-675$04.50/0

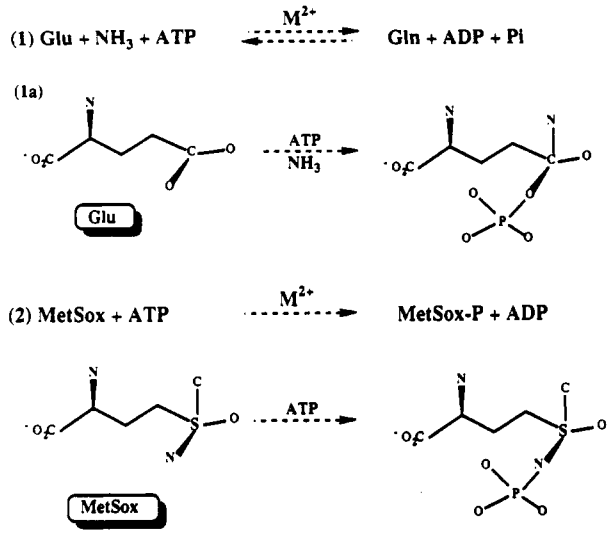

FIGURE 1: Three reactions catalyzed by GS. Reaction 1 is the biosynthetic reaction; reaction 1a is the formation of the tetrahedral transition state intermediate. Reaction 2 is the irreversible inhibition of GS by MetSox.

X-ray crystallography is well suited for defining these interactions. In previous work, X-ray methods were used to determine a 3.5-Å atomic model for 5616 amino residues of dodecameric unadenylylated GS from *Salmonella typhimurium* (Almassy et al., 1986; Yamashita et al., 1989) and 2.8-Å refined models for both *S. typhimurium* and *Escherichia coli* GS (Liaw, 1992; Liaw et al., 1993a). GS from *S. typhimurium* and from *E. coli* consists of 12 identical subunits with 622 symmetry, arranged as two face-to-face benzene rings. The active sites are located at the interfaces of subunits in the same ring, in funnel-shaped cavities, about 30 Å wide at the top of the GS molecule, 15 Å wide at the middle, 10 Å wide at the bottom, and 45 Å deep, which are open at both the top and the bottom. About halfway down each active site is a shelf formed by the two metal ions and their ligands. These metals are required for the enzyme activity; the more tightly binding site is termed n_1, and the less tightly binding site is called n_2 (Denton & Ginsburg, 1969). The 2.8-Å native GS model is used here, along with Fourier maps of five GS complexes to infer structural aspects of the enzyme mechanism.

MATERIALS AND METHODS

Crystal Soaking. Fully unadenylylated GS from *S. typhimurium* was isolated by ammonium sulfate precipitation and by a Cibracon Blue affinity column (Liaw, 1992). Crystals were grown by the hanging drop method of vapor diffusion (Liaw et al., 1993b). An effector was dissolved in synthetic mother liquor and added to the crystal drops (Liaw et al., 1993c). Estimated final concentrations of L-Glu, L-Gln, MetSox, ADP, and AMPPNP were 10, 20, 2, 1.3, and 1.3 mM, respectively. X-ray data of these GS–effector complex crystals (see Table 1) were collected with a RAXIS-II image plate detector (Rigaku). All of these complex crystals were isomorphous with respect to the native GS crystals, having space group *C*2 and unit-cell dimensions a = 235.5 Å, b = 134.5 Å, c = 200.1 Å, and β = 102.8°.

Averaged Fourier Maps. Fourier difference maps, using Fourier coefficients ($F_{o_{GS-effector}} - F_{o_{GS}}$), ($F_o - F_c$), and ($2F_o - F_c$), all 12-fold averaged, were calculated by CCP4 [a suite of program for protein crystallography (SERC, Daresburg Laboratory, Warrington, England] and X-PLOR (Brünger, 1993) programs implemented on a DEC VAX 4000 at UCLA. Phases of the 2.8-Å native GS model were used as phases of the complexes, as justified by the crystal isomorphism. ($F_{o_{GS-effector}} - F_{o_{GS}}$) maps were used to define effector binding sites and large conformational changes; ($2F_o - F_c$) maps with phases computed from the model, omitting specific regions of interest, were used to detect small but significant conformational changes in these regions, and ($F_o - F_c$) maps were used to check changed positions of amino acid residues. The Fourier maps display little noise above the 1σ contour level (except the difference map of GS–AMPPNP), perhaps because of the 12-fold averaging. The poorer quality of the ($F_{o_{GS-AMPPNP}} - F_{o_{GS}}$) map may be due to inferior X-ray data (a high R merge of 17%), or perhaps because of numerous charges nearby the metal ions and their ligands (Liaw et al., 1993a). However, all ($2F_o - F_c$) maps are clean, perhaps because of the improved atomic model (S.-H. Liaw and D. Eisenberg, manuscript in preparation).

Table 1: Summary of X-ray Data for GS-Effectors

crystal	resolution (Å)	unique/ total reflections	R_{sym}[a]	$\langle\Delta F\rangle/\langle F\rangle$[b]
GS–Glu	2.8	110184/170218	6.0%	17.8%
GS–MetSox	2.9	116044/355084	8.5%	13.5%
GS–Gln	2.8	102472/155698	6.9%	12.6%
GS–ADP	2.8	86071/126045	7.2%	16.1%
GS–AMPPNP	3.0	74798/107472	17.9%	20.4%

[a] On intensity. A measure of the precision of data collection. [b] Mean fractional isomorphous difference $(\Sigma||F_{PH}| - |F_P||)/(\Sigma|F_P|)$.

RESULTS

Model Building of Effectors. Individual atomic groups are not well resolved at 2.8-Å resolution, but we have been able to build plausible models of effectors bound to GS from overall shapes and chemical reasoning. The strongest peaks in the difference maps of GS–Glu, GS–Gln, and GS–MetSox at the 2σ contour level appear at the same position at the bottom of the active site funnel, just below the n_1 Mn^{2+}. And the strongest peaks in the maps of GS–ADP and GS–AMPPNP at the 1σ contour level are adjacent to the n_2 Mn^{2+}, above the Glu site in the funnel. Overlapping density peaks show that MetSox and Gln bind at the L-Glu binding site, whereas ADP binds to the ATP site. Atomic models of the effectors L-Glu, L-Gln, L-MetSox, ADP, and AMPPNP were built into the strongest density peak in their respective difference maps (Figure 2).

Similarly, models of GS–Glu, GS–Gln, and GS–MetSox were built. In previous crystallographic work (Liaw et al., 1993c), the feedback inhibitor Gly was found to bind within the active site at the Glu site. The shape of the density peak of Gly revealed its orientation. In this orientation, its carboxylate group can accept hydrogen bonds from Arg 321, and its ammonium group can donate hydrogen bonds to the carbonyl group of Gly 265 and the carboxylate side chain of Glu 131. This permitted models for the "main chain" of L-Glu, L-MetSox, and L-Gln to be built at the same positions as that of Gly. The side chain of L-Glu was built into elongated electron density extending toward the ATP binding site, which places it in position for the formation of γ-glutamyl phosphate in the biosynthetic reaction (Figure 4a). The two carboxylate groups of Glu are unlikely to interchange positions in our model because both the carboxylate and ammonium ions of the "main chain" of Gly, Ala, Ser, and Glu contribute to binding to GS. On the basis of the height of the density peaks,

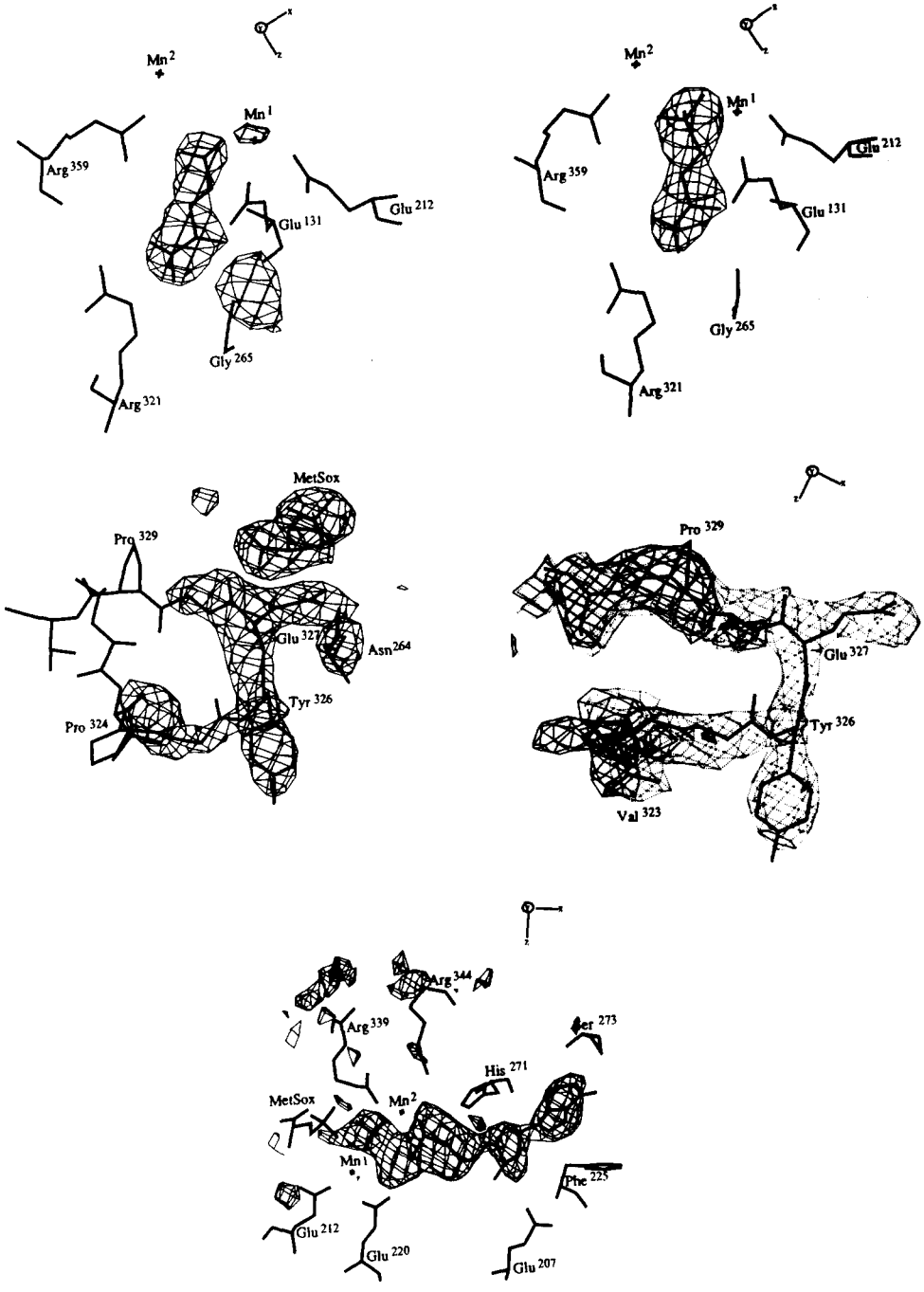

FIGURE 2: Model building of effectors in 12-fold averaged Fourier difference maps, ($F_{oGS-effector} - F_{oGS}$) before refinement. (a, top left) ($F_{oGS-Glu} - F_{oGS}$); (b, top right) ($F_{oGS-MetSox} - F_{oGS}$); (e, bottom) ($F_{oGS-ADP} - F_{oGS}$). The difference map of GS–Gln is similar to that of GS–Glu, and that of GS–AMPPNP is similar to that of GS–ADP. (c, middle left) The difference map ($F_{oGS-MetSox} - F_{oGS}$) in greater detail, but from a different point of view than panel b. (d, middle right) The ($2F_o - F_c$) map of the native GS is shown in solid lines and that of GS–MetSox in dotted lines. In the native GS ($2F_o - F_c$) map, virtually no density is observed for residues 325–328. However, the electron density for these residues is seen in the map of the GS–MetSox complex, indicating that these residues become more ordered upon binding of the inhibitor MetSox. The relative orientation of the different views is indicated by the crystallographic axes. The GS 6-fold axis is parallel to z.

interactions of the "main chains" of Glu, Gln, and MetSox with GS are stronger than interactions of the side chains with GS.

MetSox was positioned, as Glu, with its elongated side chain toward the ATP site. Its sulfoximine nitrogen atom must be oriented toward the ATP site, because this nitrogen is phosphorylated as shown by Rowe et al. (1969). Once this nitrogen atom is oriented, the positions of all atoms of the *S*-sulfoximine group are defined: the oxygen toward Arg 339 and Arg 359; and the methyl group toward Glu 327 and Asp 50′ of the adjacent subunit. By analogy with MetSox, we orient the amide oxygen atom of L-Gln toward Arg 359 and Arg 339, and the amide nitrogen toward the n_1 metal ion and the phosphate site (Figure 4d).

Conformational Changes Induced by MetSox Binding. In the difference map of GS–MetSox, in addition to the strongest peak which we interpret as the MetSox, there is a positive density peak and a negative peak on opposite sides of Asn 264 (Figure 2c). These two peaks can be interpreted as the movement of Asn 264 away from the MetSox site and toward the ϵ-amino group of Lys 176. This movement of the amide group of Asn 264 is also observed in the structures of GS–Glu, GS–Gln, GS–Ser, GS–Gly, and GS–Ala (Liaw et al., 1993c).

FIGURE 3: Funnel-shaped active site viewed from the outside of the GS dodecamer with the noncrystallographic six-fold (z-axis) vertical [drawn by the program Molscript (Kraulis, 1991)]. The active site barrel is constituted by two adjacent subunits. The front chains are darker than the ones behind. The shaded fragment containing K 47′ is part of the adjacent subunit. ATP enters from the top, and Glu enters from the bottom of the funnel. The two metal ions and their ligands form a shelf that separates these two substrates. Shown in very dark shading, containing E 327 and the residues 324–328, is the Glu binding flap. Glu 327, of which atoms are shown below the substrate Glu, is stabilized by MetSox binding, blocking the Glu entry.

The next strongest postive peaks and negative peaks in the difference map, ($F_{o_{GS-MetSox}} - F_{o_{GS}}$), are along residues 322–329; these show that residues 324–328 become more ordered upon MetSox binding (Figures 2c and 4c). There is little electron density for these residues in the averaged ($2F_o - F_c$) map of native GS, but there is density in the map of GS–MetSox, especially around Glu 327 (Figure 2d). In our studies of 15 GS difference maps, the ($2F_o - F_c$) map of GS–MetSox is the only one having electron density for the side chain of Glu 327 (Figure 2d). Interaction of the sulfoximine group of MetSox with the γ-carboxylate grop of Glu 327 may stabilize residues 324–328. However, these residues are not similarly stabilized in the complexes GS–Glu, GS–Gln, GS–(Glu+NH_4^+), GS–ADP, or GS–AMPPNP.

Functions of Residue Glu 327 and Segment 324–328. This segment resides at the intersubunit contact, with Glu 327 separated from Ser 52′ and Ser 53′ of the adjacent subunit by 4 and 3.4 Å, respectively. It may be by this interaction that MetSox increases the intersubunit stability of GS molecules (Maurizi & Ginsburg, 1982). Also from the crystal structure of GS–MetSox, it is apparent that this segment forms a Glu binding flap at the bottom of the active site cavity. Glu binds to GS–Mn and GS–Mn–ATP through this flexible loop. However, stabilization of this loop by MetSox blocks Glu entry from the bottom of the active site (Figure 3), which may account in part for the strong binding and inhibition of GS activity by MetSox. Furthermore, stabilization of Glu 327 by MetSox implies that Glu 327 may be also stabilized by the tetrahedral transition-state intermediate in catalysis. There may be a salt bridge between the side chain of Glu 327 and the γ-amino group of the tetrahedral intermediate (Figure 4c). Finally, the side chain of Glu 327 is only 2.6 Å distant from the methyl group of MetSox. This methyl group in MetSox is the analog of the ammonium ion of the transition-state complex. This suggests that Glu 327 may enhance ammonium ion binding at this site or/and perhaps accept a proton from the ammonium ion or from the γ-amino group

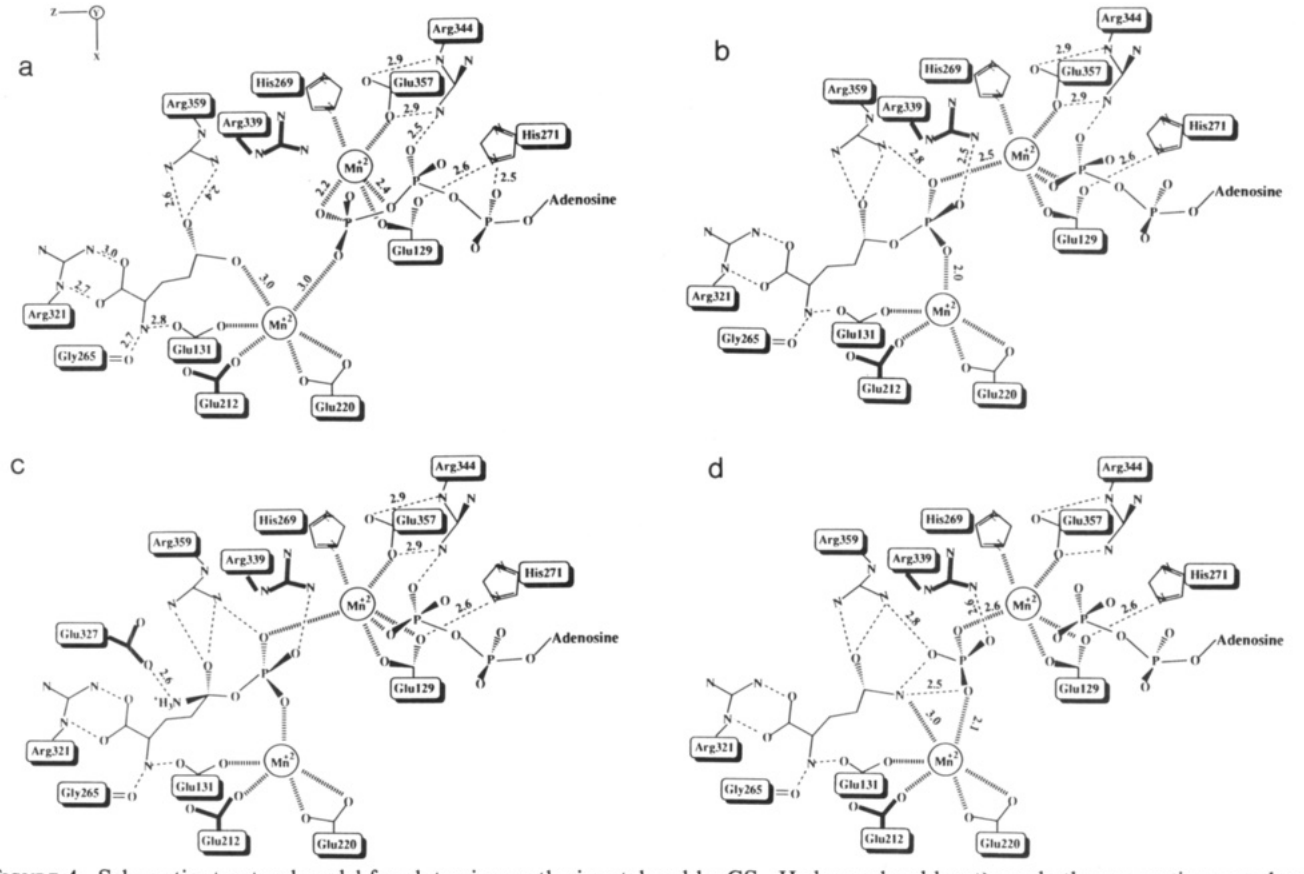

FIGURE 4: Schematic structural model for glutamine synthesis catalyzed by GS. Hydrogen bond lengths and other separations are shown by numbers (see text).

of the tetrahedral intermediate. This suggestion from the protein model of participation of ammonium ion binding by Glu 327 has been confirmed by protein engineering studies: replacement of Glu 327 by Ala increases the K_m values of ammonium ion, from 0.1 to 2.5 mM in the presence of Mn^{2+} and from 0.1 to 12.8 mM in the presence of Mg^{2+} (Alibhai & Villafranca, 1994). In short, Glu 327 may be part of the ammonium binding site on GS.

Interpretation of the Difference Map, ($F_{oGS-ADP} - F_{oGS}$). Interpretation of the ($F_{oGS-ADP} - F_{oGS}$) map (Figure 1e) by itself is complicated because the difference density appears somewhat too large for ADP. However, the ($2F_o - F_c$) and ($F_o - F_c$) maps calculated with the native phases display a peak of size appropriate for ADP, two water molecules, and one phosphate. The ADP model is described more fully in a forthcoming paper.[2] The source of P_i in the ADP difference map is from the crystallization mother liquor which contains 0.3 mM phosphate. The weak P_i peak appears only in the presence of ADP, consistent with the observation that ADP can enhance P_i binding to GS–Mn (Rhee & Chock, 1976). The two water molecules are probably associated with the phosphate and metal ions: it is common for water molecules to serve as ligands for metal ions, thereby enhancing structural stability of the protein, and to participate in catalytic steps. One putative water is 2.5 Å from the β-phosphate oxygen of ADP, 2.7 Å from the carboxylate oxygen of Glu 220, and 4 Å from the n_1 ion. The other putative water is 2.5 Å away from the P_i oxygen atoms, 3.5 Å from Glu 212, and 3 Å from the n_i ion. This second water molecule is replaced by Glu, Gln, and MetSox as they bind to GS because they occupy the same site. Consistent with this interpretation are EPR and NMR studies which showed that there are two water molecules ligating the n_1 ion one of which is replaced by MetSox (Eads et al., 1988). The ADP difference map also shows that ADP binding displaces Glu 129 toward the n_2 ion, His 269, and His 271. This may be because of the proximity of the β-phosphate group to Glu 129 (Figure 4b). The P_i was placed in difference density between the Gln site and the ATP site. In this position, metal ions, Arg 339, and Gln could stabilize P_i binding for the reverse biosynthetic reaction, as well as for Gln hydrolysis, and for the glutamyl transfer reaction. Adenosine rings of AMPPNP and ADP were built into their difference density peaks in the same way as that of AMP.[2] The β- and γ-phosphate groups serve as ligands for the metal ions (Figure 4a,b).

Effects of the Binding of ADP and AMPPNP. Examination of electron density maps suggests that the GS–Mn–ADP complex may be more stable than GS–Mn–AMPPNP. ADP binding, but not AMPPNP, increases intersubunit interactions within the same ring around the active site cavities: the amino acid residues located at the intersubunit contacts, residues 61–64 and 337–340, are stabilized upon ADP binding, as judged by stronger densities on the ($2F_o - F_c$) maps and Arg 344 interacting with Asp 64′, and Arg 339 with Asp 50′. Second, the binding of ADP and AMPPNP induces Arg 359 movement toward the γ-carboxylate oxygen of substrates Glu and Gln and toward the sulfoximine oxygen of MetSox (from 3.6 and 2.6 Å). These movements would be expected to enhance the binding to GS of Glu, Gln, and MetSox, and in fact this enhancement is seen directly in dissociation constants (Rhee & Chock, 1976; Ginsberg et al., 1987). Third, the presence of ADP but not AMPPNP induces Arg 339 movement toward the P_i site. This movement might assist phosphoryl transfer and P_i binding (Figure 4b,d). The increased phosphate binding by ADP is inferred by the presence of P_i in the ADP difference map (Figure 2e) and by dissociation constants. Fourth is the movement of Asp 50′ toward the site of the methyl group of MetSox (from 4.2 to 2.6 Å) induced by ADP binding, but not AMPPNP. This implies that the ammonium ion binding site is created after the formation of γ-glutamyl phosphate and ADP. Thus this motion of Asp 50′ is consistent with the conclusion from studies of GS inhibition by MetSox (Weisbrod & Meister, 1973) that Gln synthesis catalyzed by GS is not a concerted reaction. Similarly, the greater effectiveness of ADP in catalyzing Gln hydrolysis and γ-glutamyl transfer, compared to ATP or AMP (Levintow & Meister, 1954), can be explained by the enhancement of P_i binding, of phosphoryl transfer, and of hydroxylamine binding because of the conformational changes induced by ADP binding. Furthermore, the proximity of the negatively charged P_i to the negatively charged Glu and to the negatively charged γ-phosphate of ATP explains why P_i and Glu, or P_i and ATP, have negatively cooperative effects in binding to the enzyme (Shrake et al., 1978).

Substrate Entries. The crystal structures of GS and GS–effector complexes reveal that ATP and Glu each has its own entry to the funnel-shaped active-site cavity (Figure 3). ATP has an entry, roughly 30 Å wide, which is nearly parallel to the noncrystallographic 6-fold axis and is open to the top of the molecule (for the subunits on the upper layer). The Glu entry is smaller and extends upward from the bottom of the subunit junction and is guarded by residues 324–328, the Glu binding flap. The two metal ions and their ligands form a shelf in the active site that separates the ATP entry above from the Glu entry below. This shelf lies roughly 23 Å below the ATP entrance. That is, Glu cannot enter from the top (Figure 3). Furthermore, inactivation of GS by covalent modification of Lys 47 with the ATP analogue 5′-*p*-fluorosulfonylbenzoyladenosine (FSBA) (Pinkofsky et al., 1984) may be due to blocking ATP entry because Lys 47 of the adjacent subunit is located in the vestibule of the ATP entry.

DISCUSSION

Proposed Ammonium Ion Binding Site. MetSox was suggested by Weisbrod and Meister (1973) as a transition-state analog with its methyl group occupying the same position as the γ-amino group of the tetrahedral intermediate (Figure 1). Thus an ammonium ion binding site might be expected to lie near to the methyl group of MetSox and along the direction of the bond from the sulfur atom to the methyl group. Because this position within the structure is polar and solvent-exposed, an ammonium ion appears to be a better candidate than an ammonia molecule for initial binding to GS. Also, hydroxylamine is as good a substrate for GS as ammonia whereas methylamine, a less polar amine, is a poor substrate (Colanduoni et al., 1987). In our model, Glu 327, Glu 212, Tyr 179, and Asp 50′, and Ser 53′ of the adjacent subunit, are all within 5 Å of the methyl group of MetSox. An ammonium ion could occupy this site and donate hydrogen bonds to Glu 327, Tyr 179, Ser 53′, and Asp 50′.

The amino acid residues involved in the specific binding of an ammonium ion, as proposed from the structure of GS–MetSox, have been confirmed by studies of engineered residue replacements by Villafranca and co-workers. Replacement of Asp 50′ with Ala increases the K_m of ammonia 500-fold. The similar K_m for ammonia of the mutant D50E implies importance of the negative charge at this residue for the ammonium ion binding. Replacement of Glu 327 with Ala

[2] S.-H. Liaw, J. Gyo and D. Eisenberg, manuscript in preparation.

Scheme 1

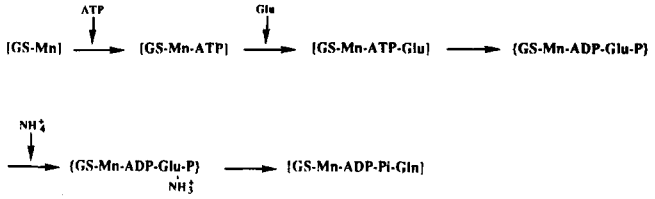

also increases the K_m of ammonium ion (Alibhai & Villafranca, 1994). Moreover, studies of pH-dependent enzyme catalysis and substrate binding by Colanduoni et al. (1987) suggested that the substrate ammonia must be deprotonated by a base for the catalytic reaction to occur.

Enzymatic Mechanism of Glutamine Synthesis. On the basis of the structural studies described here, we can build on earlier proposals for the catalytic mechanism of Gln synthesis catalyzed by GS. Our tentative mechanism is the following (see Scheme 1): First, ATP and L-Glu bind to GS in order because ATP binding to GS enhances Glu binding (Figure 4a). Second, the two enzyme-bound metal ions, especially the n_2 ion, polarize the γ-phosphate of ATP making the γ-phosphorus atom more positive, promoting Glu to attack to produce γ-glutamyl phosphate. The two positively charged metal ions and Arg 339 participate in phosphoryl transfer (Figure 4b). Third, movement of Asp 50′ of the adjacent subunit is induced by the presence of ADP, forming the ammonium ion binding site. The side chain of Asp 50′ is then positioned to accept a proton from the bound ammonium ion, forming ammonia, which can attack the γ-glutamyl phosphate to yield a tetrahedral intermediate. This tetrahedral intermediate can stabilize residues 324–328 by forming a salt link to the negatively charged side chain of Glu 327 from the positively charged γ-amino group of the tetrahedral intermediate (on the basis of GS–MetSox). This blocks Glu exit (Figure 4c). Finally, the phosphate group of the transitary tetrahedral intermediate leaves, and Glu 327 accepts a proton, perhaps from the γ-amino group of the intermediate, to yield Gln. The amide nitrogen of Gln hydrogen-bonds to the n_1 ion and P_i (Figure 4d). The absence of interaction of the product Gln with Glu 327 releases the flexible segment (324–328), permitting Gln to diffuse from the active site and allowing Glu to enter for the next catalytic cycle.

Ordered Substrate Binding Mechanism. EPR and binding studies have established that GS binds its substrates near its two metal ion sites (Hunt et al., 1975; Eads et al., 1988). What is less clear is the order of substrate binding. Fluorometric studies suggested that substrates bind to GS in random order (Timmons et al., 1974; Rhee et al., 1976). In contrast, kinetic analysis (Meek & Villafranca, 1980) and isotope-exchange enhancement studies (Clark & Villafranca, 1985) suggested an order of substrate binding. The structures of GS–ADP, GS–AMPPNP, and GS–MetSox argue for an ordered pathway because the binding of ADP and AMPPNP induces movement of Arg 359 to form more fully the binding sites for Glu, Gln, and MetSox and because the putative ammonium ion site forms after ADP and γ-glutamyl phosphate binding. Thus the preferred order of addition substrates is ATP, then Glu, and then an ammonium ion (Scheme 1).

Evolutionary Data Supporting This Reaction Mechanism. Alignment of GS amino acid sequences from mammals, plants, and bacteria using the GAP program by Shatters and Kahn (1989) reveals that all amino acid residues involved in our proposed mechanism (Asp 50, Glu 129, Glu 131, Glu 212, Glu 220, Gly 265, His 269, Arg 321, Glu 327, Arg 339, Arg 344, Glu 357, and Arg 359) are invarient even though the amino acid identity between enzymes is only 20%. This implies that functional and structural aspects of the active site of GS are conserved in mammals, plants, and bacteria. This conservation is consistent with identical reaction mechanisms in prokaryotic and eukaryotic GS.

Exchange Reactions. Our proposed reaction mechanism is also consistent with, and offers explanations for, a number of the findings by Boyer and co-workers who studied the exchange reactions of adenylylated *E. coli* GS. First, the requirement of ADP binding to create the ammonium ion binding site explains why a Glu $\leftrightarrow$ NH_3 exchange could not be observed in the absence of ADP (Welder & Boyer, 1972a). Second, the block of the ATP $\leftrightarrow$ P_i exchange but not the Glu $\leftrightarrow$ Gln exchange by GDP and AMP (Welder & Boyer, 1972b) correlates nicely with our separate channels for ATP–ADP and Glu–Gln entry and release. The binding of GDP and AMP in the ATP channel completely inhibits the ATP $\leftrightarrow$ P_i exchange which is supported by our X-ray data which show GDP and AMP to bind at the ATP site.[2] Similarly, the ability of alanine and glycine to block completely the Glu $\leftrightarrow$ Gln exchange (Welder & Boyer, 1972b) is consistent with the blocking of Glu and Gln binding to GS by the binding of alanine and glycine in the Glu–Gln channel (Liaw et al., 1993c).

Arsenolysis of Glutamine. Our structure-based model for the biosynthesis of Gln is also compatible with the other reactions catalyzed by GS: γ-glutamyl transfer, glutamine hydrolysis, and glutamine arsenolysis. Arsenate is believed to bind at the P_i site because it is a competitive inhibitor with phosphate (Meek & Villafranca, 1980). As in the reversal of Gln synthesis with P_i replaced by arsenate, Glu formation may be through an unstable arsenate intermediate (Levintow & Meister, 1954). We speculate that the arsenate oxygen attacks Gln to form an unstable acyl arsenate with concomitant release of ammonia. Formation of an acyl phosphate was proposed in the reverse biosynthetic reaction by Clark and Villafranca (1985). Then deprotonation of one water molecule perhaps by Asp 50′ leads a hydroxyl ion to replace the arsenate group of γ-glutamyl arsenate to yield glutamate. In the same way, hydroxylamine replaces the arsenate group of γ-glutamyl arsenate to yield glutamylhydroxamate. Ammonium ion, hydroxylamine, and water may bind at the same site for attacking the γ-glutamyl phosphate in their respective reactions: the biosynthetic reaction, the γ-glutamyl transfer reaction, and the hydrolysis of glutamine. Also, these three molecules may not bind to this site until GS has bound ADP and the γ-glutamyl phosphate. In summary, the GS–Mn–γ-glutamyl phosphate–ADP complex is the common intermediate in these three reactions, and formation of the respective product (Gln, Glu, or glutamylhydroxamate) is determined by the attacked molecule (ammonia, water, or hydroxylamine). Thus, Gln synthesis and Gln hydrolysis are dependent on competition of the binding of ammonium ion and of water to the common intermediate, the binding affinity, and the concentration of an ammonium ion. The positively charged ammonium ion binds to GS more strongly than water because of the negatively charged residues surrounding the ammonium binding site, Glu 327 and Asp 50′, as shown by the low K_m of ammonium ion, 0.1 mM (Meek & Villafranca, 1980). Also, we would expect that at low ammonia concentrations many reaction reversals occur before Gln is released but at high ammonia concentrations no reversals occur. This is exactly what has been observed by Bild and Boyer (1980).

Functions of Divalent Cations on GS Activity. On the basis of crystal structures of GS complexes reported here, we believe

the two bound metal ions serve three functions in enzymatic catalysis (Figure 4): the binding of substrates, the transfer of the phosphate group, and structural stability (Liaw et al., 1993a). The metal ion at the n_1 site interacts with Glu or with Gln directly as well as with MetSox without water mediation, a modification of earlier proposals based on NMR studies (Balakrishnan & Villafranca, 1978). The metal ion at the n_2 site participates in the binding of ADP and ATP but not AMP. The incompletely satisfied positive charge of the n_2 ion with groups on GS causes a higher binding affinity of ATP to GS (Liaw et al., 1993a) and draws electrons from the γ-phosphorus atom toward the metal ion to increase the susceptibility of the phosphorus atom to the nucleophile, Glu.

ACKNOWLEDGMENT

We thank Drs. Joseph J. Villafranca and Murtaza F. Alibhai for helpful discussion and for studies of the mutants of Asp 50, Tyr 179, and Glu 327, related to the GS mechanism, Drs. Paul D. Boyer, David Sigman, and Robert J. Almassy for discussion, and NIH for support.

REFERENCES

Alibhai, M. F., & Villafranca, J. J. (1994) *Biochemistry* (following paper in this issue).
Almassy, R. J., Janson, C. A., Hamlin, R., Xuong, N.-H., & Eisenberg, D. (1986) *Nature 323*, 304–309.
Balakrishnan, M. S., & Villafranca, J. J. (1978) *Biochemistry 17*, 3531–3538.
Bild, G. S., & Boyer, P. D. (1980) *Biochemistry 19*, 5774–5781.
Brünger, A. T. (1992) X-PLOR, version 3.0, Yale University Press, New Haven, CT.
Clark, D. D., & Villafranca, J. J. (1985) *Biochemistry 24*, 5147–5152.
Colanduoni, J., Nissan, R., & Villafranca, J. J. (1987) *J. Biol. Chem. 262*, 3037–3043.
Cooper, A. J. L., & Plum, F. (1987) *Physiol. Rev. 67*, 440–519.
Denton, M. D., & Ginsburg, A. (1969) *Biochemistry 8*, 1714.
Derouiche, A., & Frotscher, M. (1991) *Brain Res. 552*, 346–350.
Eads, C. D., LoBrutto, R., Kumar, A., & Villafranca, J. J. (1988) *Biochemistry 27*, 165–170.
Ginsburg, A., Gorman, E. G., Neece, S. H., & Blackburn, B. (1987) *Biochemistry 26*, 5989–5996.
Hunt, J. B., Smyrniotis, P. Z., Ginsburg, A., & Stadtman, E. R. (1975) *Arch. Biochem. Biophys. 166*, 102–124.
Kraulis, P. J. (1991) *J. Appl. Crystallogr. 24*, 946–950.
Levintow, L., & Meister, A. (1954) *J. Biol. Chem. 209*, 265–280.
Liaw, S.-H. (1992) Ph.D. Thesis, University of California, Los Angeles.
Liaw, S.-H., Villafranca, J., & Eisenberg, D. (1993a) *Biochemistry 32*, 7999–8003.
Liaw, S., Jun, G., & Eisenberg, D. (1993b) *Protein Sci. 2*, 470–471.
Liaw, S., Pan, C., & Eisenberg, D. (1993c) *Proc. Natl. Acad. Sci. U.S.A. 90*,. 4996–5000.
Maurizi, M. R., & Ginsburg, A. (1982) *J. Biol. Chem. 259*, 7246–7251.
Maurizi, M. R., & Ginsburg, A. (1986) *Biochemistry 25*, 131–140.
Meek, T. D., & Villafranca, J. J. (1980) *Biochemistry 19*, 5513–5519.
Meister, A. (1974) in *The Enzymes* (Boyer, P., Ed.) *10*, 669–754.
Meister, A. (1980) in *Glutamine: Metabolism, Enzymology, and Regulation of Glutamine Metabolism* (Palacios, R., & Mora, J., Eds.) pp 1–40, Academic Press, New York.
Pinkofsky, H. B., Ginsburg, A., Reardon, I., & Heinrikson, R. L. (1984) *J. Biol. Chem. 259*, 9619–9622.
Rhee, S. G., & Chock, P. B. (1976) *Biochemistry 15*, 1755–1760.
Rhee, S. G., Chock, P. B., & Stadtman, E. R. (1976) *Biochimie 58*, 35–49.
Rowe, W. B., Ronzio, R. A., & Meister, A. (1969) *Biochemistry 8*, 2674–80.
Shatters, R. G., & Kahn, M. L. (1989) *J. Mol. Evol. 29*, 422–428.
Shrake, A., Parak, R., & Ginsburg, A. (1978) *Biochemistry 17*, 658–664.
Stadtman, E. R., & Ginsburg, A. (1974) in *The Enzymes* (Boyer, P., Ed.) *10*, 755–807.
Timmons, R. B., Rhee, S. G., Luterman, D. L., & Chock, P. B. (1974) *Biochemistry 13*, 4479–4485.
Wedler, F. C., & Boyer, P. D. (1972a) *J. Biol. Chem. 247*, 984–992.
Wedler, F. C., & Boyer, P. D. (1972b) *J. Biol. Chem. 247*, 993–1000.
Weisbrod, R. E., & Meister, A. (1973) *J. Biol. Chem. 248*, 3997–4002.
Whitley, E. J., Jr., & Ginsburg, A. (1980) *J. Biol. Chem. 255*, 10663–10670.
Yamashita, M. M., Almassy, R. J., Janson, C. A., Cascio, D., & Eisenberg, D. (1989) *J. Biol. Chem. 264*, 17681–17690.